Ground Water Monitoring&Remediation

# Evidence for Instantaneous Oxygen-Limited Biodegradation of Petroleum Hydrocarbon Vapors in the Subsurface

*by G.B. Davis, B.M. Patterson, and M.G. Trefry*


## Abstract

Petroleum hydrocarbon vapors biodegrade aerobically in the subsurface. Depth profiles of petroleum hydrocarbon vapor and oxygen concentrations from seven locations in sandy and clay soils across four states of Australia are summarized. The data are evaluated to support a simple model of biodegradation that can be used to assess hydrocarbon vapors migrating toward built environments. Multilevel samplers and probes that allow near-continuous monitoring of oxygen and total volatile organic compounds (VOCs) were used to determine concentration depth profiles and changes over time. Collation of all data across all sites showed distinct separation of oxygen from hydrocarbon vapors, and that most oxygen and hydrocarbon concentration profiles were linear or near linear with depth. The low detection limit on the oxygen probe data and because it is an in situ measurement strengthened the case that little or no overlapping of oxygen and hydrocarbon vapor concentration profiles occurred, and that indeed oxygen and hydrocarbon vapors were largely only coincident near the location where they both decreased to zero. First-order biodegradation rates determined from all depth profiles were generally lower than other published rates. With lower biodegradation rates, the overlapping of depth profiles might be expected, and yet such overlapping was not observed. A model of rapid (instantaneous) reaction of oxygen and hydrocarbon vapors compared to diffusive transport processes is shown to explain the important aspects of the 13 depth profiles. The model is simply based on the ratio of diffusion coefficients of oxygen and hydrocarbon vapors, the ratio of the maximum concentrations of oxygen and hydrocarbon vapors, the depth to the maximum hydrocarbon source concentration, and the stoichiometry coefficient. Whilst simple, the model offers the potential to incorporate aerobic biodegradation into an oxygen-limited flux-reduction approach for vapor intrusion assessments of petroleum hydrocarbon compounds.


## Introduction

Petroleum and chlorinated vapor concentrations attenuate as they migrate toward building foundations from contaminant sources below ground surface (e.g., Johnson and Ettinger 1991). Attenuation occurs because of diffusion, controlling boundary conditions such as low vapor concentrations inside buildings and in outdoor air at the ground surface, and convection and dilution from pressure-driven air exchange in the near-surface zone of the soil profile or in the built structure (e.g., Hers et al. 2000, 2003). For petroleum hydrocarbons, in particular, there is also the potential for significant additional attenuation due to aerobic biodegradation, given the potential for oxygen to move into the subsurface from the atmosphere above ground (see, e.g., Franzmann et al. 1999; Hers et al. 2000; Roggemans et al. 2001; Davis et al. 2005; DeVaull 2007). The USEPA (2002) acknowledged this when stating that the Johnson and Ettinger (1991) model may not be applicable to petroleum hydrocarbons since it did not account for biodegradation. The scale of biodegradation can potentially reduce petroleum vapor concentrations by several orders of magnitude (Abreu and Johnson 2006). As such, excluding biodegradation from risk assessments may lead to overly conservative protective measures. For derivation of generic criteria or for screening risk assessments, several regulatory agencies in the United States (New Jersey, Massachusetts, New Hampshire, California) and Canada (Golder Associates 2008) allow attenuation factors that are derived from a model assuming no biodegradation to be adjusted downward (e.g., 10 times) to account for aerobic biodegradation. Some consideration is also being given to this in Australia (Davis et al. 2008). The adoption of such an approach and inclusion in guidelines for the assessment of contaminated sites require reliable quantification of the magnitude of aerobic biodegradation where vapor threats to human health in built environments need to be assessed.

Copyright © 2009 The Author(s)
Journal compilation © 2009 National Ground Water Association.

Laboratory and field data, along with modeling studies, are available that quantify aerobic biodegradation of petroleum hydrocarbon vapors (Franzmann et al. 1999; Hers et al. 2000; Ririe et al. 2002; Davis et al. 1998, 2005). Some models have estimated vapor biodegradation based on oxygen concentration reductions and carbon dioxide production in the subsurface (Lahvis and Baehr 1996; Davis et al. 2005). Alternatively, hydrocarbon concentration changes have been modeled without linkage to oxygen or other major gas concentrations (Trefry et al. 2001; Turczynowicz and Robinson 2001; Ririe et al. 2002). Increasingly, vapor modeling has focused on coupled hydrocarbon and oxygen transport to simulate oxygen-dependent biodegradation conditions (Öhman 1999; Hers et al. 2000; Trefry et al. 2000; Abreu and Johnson 2005, 2006; DeVaull 2007). Also, such an approach was reported earlier by Ostendorf and Kampbell (1991). In contrast, Baehr and Baker (1995) report oxygen to be nonlimiting for biodegradation where toluene was emplaced as a contaminant source in laboratory column experiments. This is at odds with most available field data and subsequent studies in the field (Lahvis and Baehr 1996). It is reasonably accepted now for modeling that oxygen transport coupled to hydrocarbon biodegradation processes is of prime importance, and that for petroleum compounds such as the BTEX (benzene, toluene, ethylbenzene, and xylene isomers) and aliphatic compounds, biodegradation is limited by oxygen availability (Hers et al. 2000; DeVaull 2007).

In many published accounts, first-order or zero-order reaction kinetics for petroleum vapors are estimated or assumed in model applications (Höhener et al. 2003; DeVaull 2007). A first-order approach assumes the rate of mass consumption is directly proportional to the concentration of the compound being consumed. Where direct linkage to the presence of oxygen is assumed (as in DeVaull [2007]), the kinetics could be better described as pseudo zero- or first-order. A zero-order approach assumes that the rate of mass consumption is constant and independent of the concentration of the compound being consumed. Ostendorf and Kampbell (1991) and Ostendorf et al. (2007) use Monod kinetics, which allows transition between zero- and first-order kinetics. Zero-order rates have often been assumed where oxygen limitations do not occur (e.g., Miller et al. 1991). However, the majority of biodegradation rates quoted in the literature are first-order. First-order rates assume the hydrocarbon (or oxygen) mass removal rate is greatest at the location of highest hydrocarbon (or oxygen) concentrations (because of its proportionality to concentration). For coupled oxygen-dependent first-order kinetics, the maximum rate is at the maximum cross-over point of the oxygen and hydrocarbon concentration profiles. Johnson et al. (1999), Hers et al. (2000), RISC (2006), and DeVaull (2007) address this in their modeling by allowing a layer where biodegradation reactions occur and by defining aerobic and anaerobic zones. Within the defined aerobic zone, first-order rates are assumed.

Here we provide evidence to support the case that aerobic biodegradation of petroleum vapors occurs only where oxygen and hydrocarbon vapor concentrations are effectively zero, i.e., at the location of their minima in the depth profile, similar to Behaviour A reported by Roggemans et al. (2001). Hence, the rate of biodegradation can be considered essentially instantaneous, i.e., rapid compared to soil vapor diffusion in the subsurface. This implies that whenever oxygen and petroleum hydrocarbons are collocated in the subsurface they react and the location at which this occurs is controlled only by the transport to that location and the stoichiometry of the reaction. This simplifies the model approach, reduces the parameter requirements, and provides a simple framework for inclusion of aerobic biodegradation into models that estimate vapor exposure. Effectively, this approximates to the flux reduction factor (FRF) concept outlined in DeVaull et al. (2002); however, these authors do not incorporate oxygen transport and also assume first-order biodegradation rather than instantaneous reactions. Data from field sites in Australia coupled with a modeling assessment are used to support the approach presented here.

## Field Sites and Methods

In Australia, seven field sites affected by petroleum hydrocarbon vapors were investigated. The site characteristics and experimental methods at two of the sites were reported in Davis et al. (2001, 2005) and Patterson and Davis (2009). Three of the sites are located in Perth, Western Australia, on sandy soils, and four are located in Queensland, New South Wales, and Victoria on clayey or silty soils. A summary of the characteristics of the sites is given in Table 1. In general, the sites range from calcareous medium to coarse sands, to fine tight clay and silty sites, with petroleum types and sources ranging from near-pure compound releases (e.g., xylene) to kerosene and gasoline, and with varying vadose zone depths ranging from 1.25 to 10 m. At each of the field sites, cores were recovered by pushing a thin-walled aluminum tube through the soil profile. For the clay soil sites, an open hole was drilled to above the required depth and then the tube was pushed through the base of the hole. The water-filled and air-filled porosities and organic carbon content of the soil were determined on subsamples. Further characteristics for each of the sites are given in Table 1.

The field sites were instrumented with multilevel samplers (MLS) and in some cases with continuous logging volatile organic compound (VOC) probes (Patterson et al. 2000) and oxygen probes (Patterson and Davis 2008). The instrumentation allowed depth profile sampling of petroleum vapor and major gas concentrations in the subsurface, and changes in concentrations, to be tracked over time. In addition, specific experiments were carried out to observe changes in vapor and major gas concentrations beneath and in the vicinity of slab-on-ground buildings and covered areas (Davis et al. 2001) and through artificial cracks placed into a slab-on-ground building (Patterson and Davis 2009).

Typically, the MLS had 0.01 to 0.10 m long screens placed at 0.05 to 1.0 m depth intervals. The MLS were fabricated from 2 mm internal diameter nylon tubing, and for the sandy sites these were bundled together and installed in a single drilled borehole. The sand was allowed to collapse around the installation or the borehole was backfilled with

**Table 1**
**Summary of Characteristics of the Seven Field Sites**

| Site Label | State of Australia | Site Setting | Soil Type | Source Type | Vadose Zone Depth (m) | Organic Carbon (% g/g) |
|---|---|---|---|---|---|---|
| A | Western Australia | Slab on ground, and open ground | Medium-coarse calcareous sand | Kerosene | ~3 | 0.16–0.97 |
| B | Western Australia | Open ground | Medium-coarse calcareous sand | Gasoline | 2.6–3.5 | 0.04–0.13 |
| C | Western Australia | Asphalt cover and open ground | Silica sand and fill over clay | Xylene and BTEX | ~3 | 0.05–1.0 |
| D | Queensland | Open ground near house | Fill over clay or clay | Gasoline | >4 | <0.01–0.22 |
| E | Queensland | Open ground near house | 0.5 m of gravel fill over clay | Gasoline | ~1.5 | 0.1–0.47 |
| F | NSW | Open ground near house | Tight brown clay and silty clay | Gasoline | 7 | 0.1–0.3 |
| G | Victoria | Open ground near house | Brown clay sand | Gasoline | 10 | <0.25–0.98 |

Note: Open ground refers to site without paved surface (i.e., vegetated or bare ground surface)

sand from the borehole. No bentonite was used. At the clay sites, for shallow depths, separate boreholes were hand augured (50 mm) for each depth interval with all boreholes located within a 0.5-m radial distance. For depths below 2 m, a rotary auger drill rig was used. Sand packing around installations followed by granular bentonite packing above the screened interval was also used at these sites to seal the installation. The MLS were sampled using glass syringes for the hydrocarbon vapors after initial purging of gas from the sampling line. Plastic syringes were used for recovering samples for major gas analyses. A minimal purge volume of three to four dead volumes was used. For the narrow diameter tubing used, the dead volume is about 3 mL/m length of tubing. Samples were analyzed for petroleum hydrocarbon vapors by gas chromatography–mass spectrometry (GC-MS) and for major gases using a GC with a thermal conductivity detector (GC-TCD).

## Results and Discussion

### Field Data

Table 2 shows data from across the seven sites. The maximum total petroleum hydrocarbon (TPH) vapor concentration was 180,000 μg/L at Site C, with 140,000 μg/L being m- and p-xylene isomers. The lowest maximum vapor concentration was 130 μg/L at Site D. Total porosities ($\theta_T$) were reasonably similar across the seven sites: individual measurements ranged from 0.30 to 0.54 $m^3/m^3$, with averages always greater than 0.38 $m^3/m^3$ (Table 2). Air filled porosities ($\theta_a$) were highly variable between sites: individual measurements ranged from effectively zero as a minimum at Sites E and F to 0.43 $m^3/m^3$ on the sandy sites. For the heavy clay/silt sites (E, F, G), the maximum individual measurement of $\theta_a$ was 0.19 $m^3/m^3$, with a maximum average of 0.14 $m^3/m^3$ at Site G and a minimum average of 0.02 $m^3/m^3$ at Site E. Effective diffusion coefficients calculated with a common tortuosity model reflected this variability.

Figure 1 shows typical total hydrocarbon vapor and major gas concentration depth profiles for Site A and Site E. At Site A, in open ground conditions (Figure 1B), oxygen concentrations decreased to approximately 1% (effectively below detection limits) at a depth of 2.5 m below ground, and total hydrocarbon vapor concentrations were above detection limits only at that depth and deeper. Carbon dioxide concentrations increased with depth and showed an approximate volume for volume replacement of oxygen over the entire depth profile. Loss of carbon dioxide is only via diffusion through to the ground surface; hence the concentrations over the greater depths were very high. At the same site under the center of a slab-on-ground building (Figure 1A), oxygen concentrations were below detection limits (approximately 1%), carbon dioxide concentrations were uniformly high, and hydrocarbon vapor concentrations were at elevated levels at the shallowest sampling port below the slab (0.15 m below ground). Note that this is only a single example of such a situation. Vapors have been shown to accumulate under the center of a ground cover at an adjacent site (Davis et al. 2001), but others have observed limited accumulation of vapors for a slab on ground building (e.g., Lundegard et al. 2008). Figure 1C shows an open ground depth profile in a heavy clay soil with 0.5 m of overlying gravel fill. In this case, the oxygen concentration was below detection limits at a depth of 1.5 m below ground, meaning that oxygen decreased to nondetect levels between 1 and 1.5 m and hydrocarbon vapor concentrations decreased from 55,000 μg/L to below the detection limits at 1 m (or again between 1 and 1.5 m).

Linear or near-linear oxygen and hydrocarbon concentration depth profiles were commonly observed (Table 2). At some sites data are limited and so linearity was difficult to infer. For example, where only two data

**Table 2**
**Characteristics for 13 Depth Profiles Observed**

| Site | Notes | $C_{H,max}$ (µg/L) | $L_{max}$ (m) | $\theta_T$ [1] ($m^3/m^3$) | $\theta_a$ [1] ($m^3/m^3$) | $D_{Ox,eff}$ [2,3] ($m^2/s$) | $D_{H,eff}$ [2,3] ($m^2/s$) | Depth profile shape |
|---|---|---|---|---|---|---|---|---|
| A | Open ground | 19000 | 2.75 | **0.51** *0.51* | **0.34** *0.34* | **2.1E-6** | *8.3E-7* | Near-linear oxygen, linear HC |
| A | Under building | 47000 | 2.25 | **0.54** *0.50* | **0.38** *0.39* | **2.6E-6** | *8.3E-7* | No oxygen, linear HC |
| B | Summer | 66000 | 2.25 | **0.52** *0.44* | **0.32** *0.38* | **1.2E-6** | *1.6E-6* | Nonlinear oxygen, linear HC |
| B | Winter: wet layer | 55000 | 2.0 | **0.54** *0.48* | **0.26** *0.35* | **7.7E-7** | *1.0E-6* | Near-linear oxygen, linear HC |
| C | Open ground | 140000 (xylene) 180000 (TPH) | 3.0 | **0.40** *0.43* | **0.30** *0.31* | **2.3E-6** | *8.7E-7* | Nonlinear oxygen, nonlinear HC |
| D | Fill: clay layer Aug 2003 | 16000 | 3.5 | **0.42** *0.50* | **0.30** *0.33* | **2.1E-6** | *7.7E-7* | Near-linear oxygen, linear HC |
| D | Fill: clay layer May 2004 | 4000 | 3.5 | **0.42** *0.50* | **0.30** *0.33* | **2.1E-6** | *7.7E-7* | Near-linear oxygen, near-linear HC |
| D | Verge Aug 2003 | 12000 | 2.3 | **0.48** *0.46* | **0.22** *0.26* | **6.0E-7** | *4.2E-7* | Near-linear oxygen, two-point linear HC |
| D | Verge May 2004 | 130 | 1.3 | **0.48** *0.46* | **0.22** *0.26* | **6.0E-7** | *4.2E-7* | Linear oxygen, low $C_{max}$ |
| E | Beside a building | 55000 | 1.5 | **0.46** *0.39* | **0.12** *0.02* | **8.3E-8** | *1.1E-10* | Linear oxygen, two-point linear HC |
| F | Apr 2002 | 6400 | 5.0 | **0.43** *0.43* | **0.11** *0.15* | **6.6E-8** | *7.4E-8* | Nonlinear oxygen, two-point linear HC |
| F | Oct 2002 | 170 | 5.0 | **0.43** *0.43* | **0.11** *0.15* | **6.6E-8** | *7.4E-8* | Nonlinear oxygen, two-point linear HC |
| G | Open ground | 72000 | 8.7 | **0.42** *0.38* | **0.14** *0.06* | **1.4E-7** | *4.7E-9* | Near-linear oxygen, near-linear HC |

$C_{H,max}$ = maximum hydrocarbon vapor concentrations, $L_{max}$ = the depth at which this occurs, $\theta_T$ = total and $\theta_a$ = air-filled porosities, $D_{Ox,eff}$ = effective oxygen and $D_{H,eff}$ = hydrocarbon vapor diffusion coefficients.
[1]Bold values are averages for the shallow oxygenated zone of the vadose zone. Italicized values are averages for the deeper vadose zone where hydrocarbon concentrations are highest.
[2]$D_{Ox,eff}$ and $D_{H,eff}$ are calculated using the Millington and Quirk (1961) approximation: $D_{eff}=D_{free}\theta_a^{10/3}/\theta_T^2$, where $D_{Ox,free}=2.01 \times 10^{-5}$ $m^2/s$ (Gliński and Stępniewski 1985), $D_{H,free}=8.0 \times 10^{-6}$ $m^2/s$ (Grathwohl 1998).
[3] Bold values are calculated from bold values of $\theta_a$ and $\theta_T$. Italicized values are calculated from italicized values of $\theta_a$ and $\theta_T$.

points were available, a two-point linear HC depth profile was noted in Table 2 (e.g., see Site E data in Figure 1C). At Sites B, C, and F, nonlinear oxygen profiles were observed, and only at Site C was a nonlinear vapor profile observed.

All oxygen and hydrocarbon vapor concentration data from each site using in situ probes, conventional manual gas sampling, and GC analyses are shown in Figure 2. The MLS data for open ground conditions were similar to profiles displayed in Figure 1B, whereas the data from beneath the center of a ground cover or slab were similar to profiles displayed in Figure 1A. For nearly all sites, oxygen concentrations were < 5% when total hydrocarbon vapor concentrations were above detection limits (i.e., > 200 µg/L for the in situ hydrocarbon probes; > 50 µg/L for the manual sampling and GC-MS analysis) and individual analytes were above detection limits (> 1 µg/L for individual analytes for the manual sampling and GC-MS analysis). Further investigation of these data and subsequent sampling showed that only oxygen data obtained by conventional manual gas sampling with GC-TCD analysis gave oxygen concentrations between 0.5% and 6% (circled data in Figure 2) when hydrocarbon concentrations were greater than 200 µg/L.

For all sites where oxygen was measured by both in situ oxygen probes and conventional manual gas sampling with laboratory GC-TCD analysis, there was reasonable agreement between the two methods for oxygen concentrations ($r^2 = 0.964$, $n = 18$); however, the linear fitted line was offset from the origin (Figure 3), suggesting either the in situ oxygen probes underestimated oxygen concentrations or the conventional manual gas sampling and GC-TCD analysis method overestimated oxygen concentrations. Laboratory calibration of the same type of oxygen probes against GC-TCD analysis as part of another study (Patterson and Davis 2008) showed a linear ($r^2 = 0.999$, $n = 8$) calibration of oxygen down to 0.22% with the line of best fit going through the origin, suggesting both the oxygen probes and GC-TCD analysis were not responsible for the offset that was observed in the field data. Oxygen contamination of soil-gas samples during manual collection or permeation of oxygen through the plastic sampling syringe during transportation to the laboratory are the likely reasons for the offset relative to the laboratory data.

Comparing only in situ oxygen probe data to manual hydrocarbon vapor data shows an even stronger relationship between the absence of oxygen and the presence of

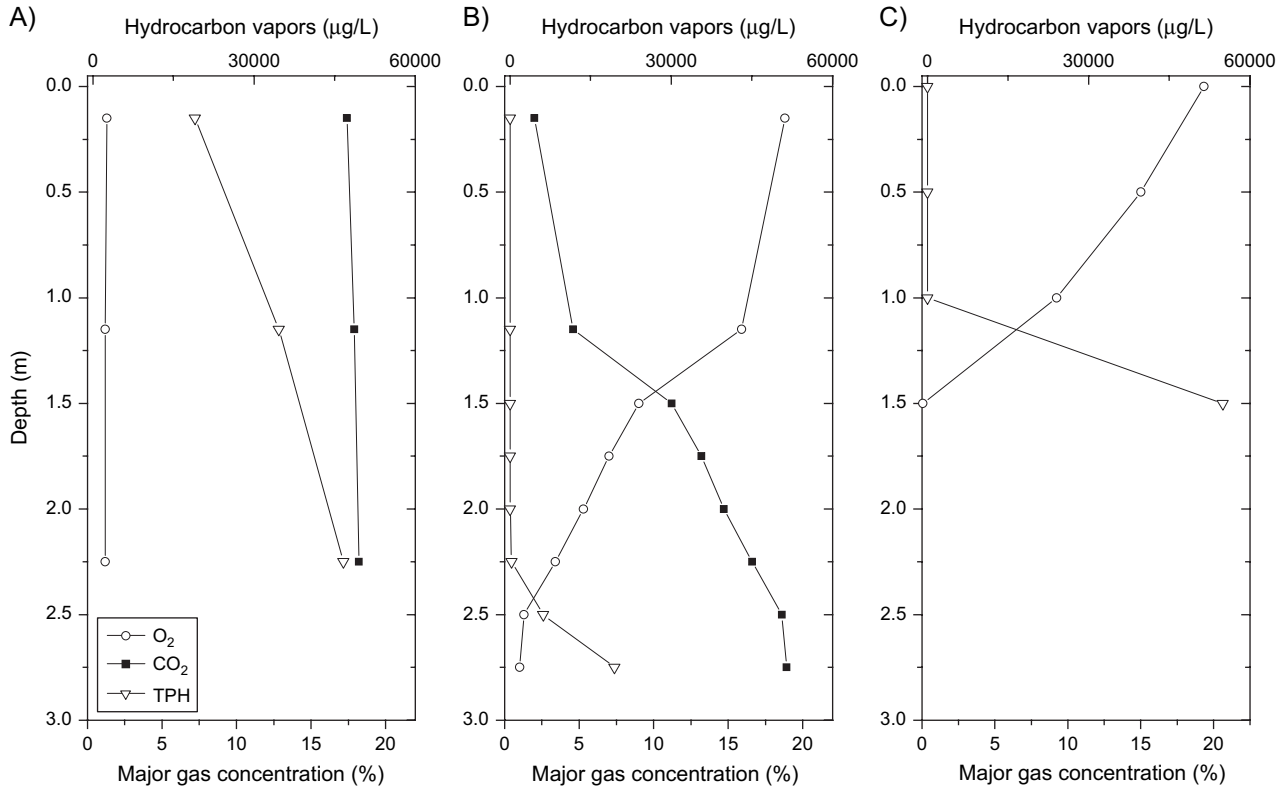


**Figure 1. Depth profiles for hydrocarbon vapor (TPH) and major gas concentrations for (A) beneath the center of a slab-on-ground building at Site A, (B) open ground conditions beside the building at Site A, and (C) open ground conditions beside the building at Site E.**

hydrocarbon vapors, and vice versa (Figure 4). The only outlier was at one depth (8.7 m) at Site G where oxygen and hydrocarbon vapors were detectable (circled data point in Figure 4). On-line monitoring showed fluctuations in oxygen concentrations that were consistent with barometric pressure changes (Figure 5), especially after a large, 80 cm diameter bore was installed within 2 to 3 m laterally of the monitoring location. These results suggest that this outlier data point was a result of oxygen ingress to this location via advective barometric pumping. Therefore, excluding the manually sampled oxygen results and the outlier at Site G, the remaining data (Figure 4) provide good evidence that there is limited overlapping of oxygen and hydrocarbon concentrations under the field conditions across these 13 depth profiles, and suggest that aerobic biodegradation of the hydrocarbon vapors occurs only in a narrow depth interval where the two intersect.

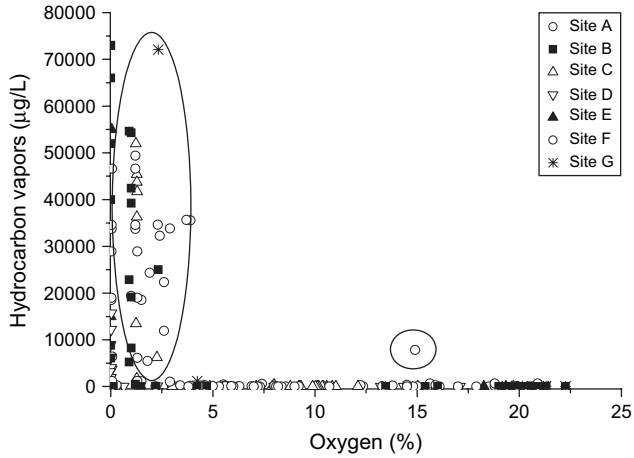


**Figure 2. Total petroleum hydrocarbon vapor concentrations compared to oxygen concentrations for Sites A-G. Circled are data from sites where at the same sampling port both oxygen and hydrocarbon vapors were above detection levels.**

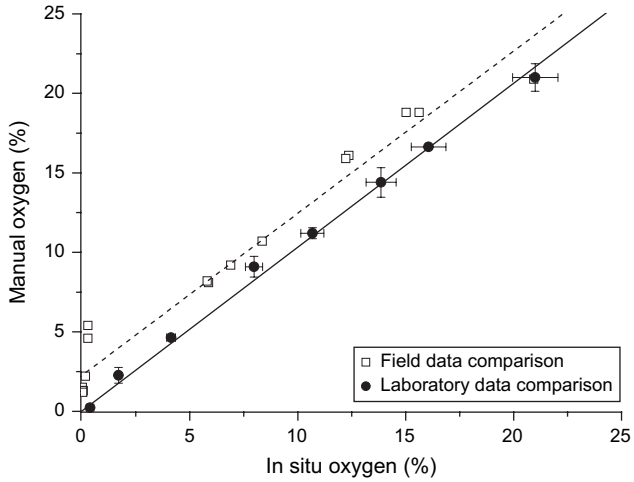


**Figure 3. Comparison of oxygen concentrations determined using in situ oxygen probes compared to data from conventional manual gas sampling with analysis by GC-TCD based on field data □ and laboratory data ●.**

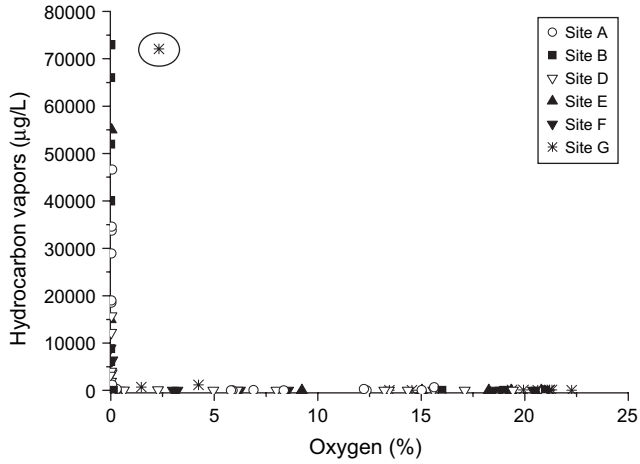


**Figure 4. Total petroleum hydrocarbon vapor concentrations compared to oxygen concentrations; data from in situ oxygen and VOC probes for all available sites.**

Confirmation of this limited overlap of oxygen and hydrocarbons concentrations can also be seen in example transient data from Site G (Figure 6). For a brief period of ~20 days, hydrocarbon vapors up to 2000 µg/L were observed at 0.5 m depth. Coincident with the presence of hydrocarbon vapors was a decreased oxygen concentration. In fact, the hydrocarbon vapor concentration time series inversely mimicked the oxygen concentration time series, providing strong evidence that the presence of even low hydrocarbon vapor concentrations can rapidly and significantly deplete subsurface oxygen concentrations. Note that no interference between the oxygen and VOC concentrations could be due to concurrent in situ logging because the in situ oxygen and hydrocarbon vapor concentrations were measured using different continuous monitoring techniques and the only commonality with the two in situ probes was the data logger that recorded probe responses.

## Instantaneous Model

The absence of significantly overlapping oxygen and vapor concentrations implies that transport of oxygen and hydrocarbon vapors to the zone of aerobic biodegradation is the rate-limiting process. Where oxygen transport is rate-limiting, some researchers (Ritchie 1977; Davis and Ritchie 1986) considered aerobic reactions to occur at a sharp interface and to be described by an oxygen front moving into the porous media over time. For this approach, Ritchie (1977) described a near-linear oxygen depth profile from ground surface to the moving reaction front. This model assumes oxygen consumption occurs only at the location of zero oxygen concentration and that this location moves progressively downward through the soil profile over time as oxygen and hydrocarbons are consumed. In this case, the source of hydrocarbon vapors is assumed finite and consumed over time, but for selected parameters the rate of movement of the zero-oxygen concentration front might be very slow. Davis and Ritchie (1986) expanded this approach to consider distributed reactions and porous media particle sizes. This led to nonlinear oxygen concentration depth profile predictions and a broader depth interval of reaction. For small particle sizes, Davis and Ritchie (1986) showed that the oxygen profile collapsed on the solution of Ritchie (1977), giving again a near-linear distribution and a narrow zone of reaction.

The approach of Davis and Ritchie (1986) identifies oxygen transport as the rate-limiting process for biodegradation, and their oxygen profiles somewhat mimic the near-linear oxygen concentration depth profiles observed at most of the sites in this study. Assuming first-order or zero-order biodegradation rates would necessarily generate nonlinear overlapping depth profiles. However, as with the earlier models that considered oxygen or hydrocarbon vapor profiles in isolation, the approach taken by Davis and Ritchie (1986) does not accommodate the coupling of

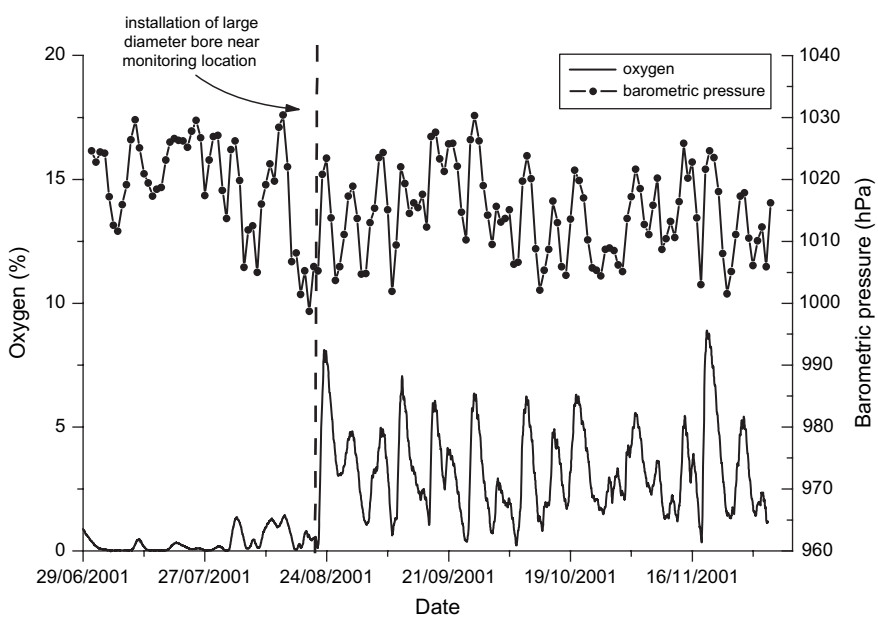


**Figure 5. Comparison of oxygen concentration responses at a depth of 8.7 m to barometric pressure variations, and the influence of an installed large-diameter borehole at Site G.**

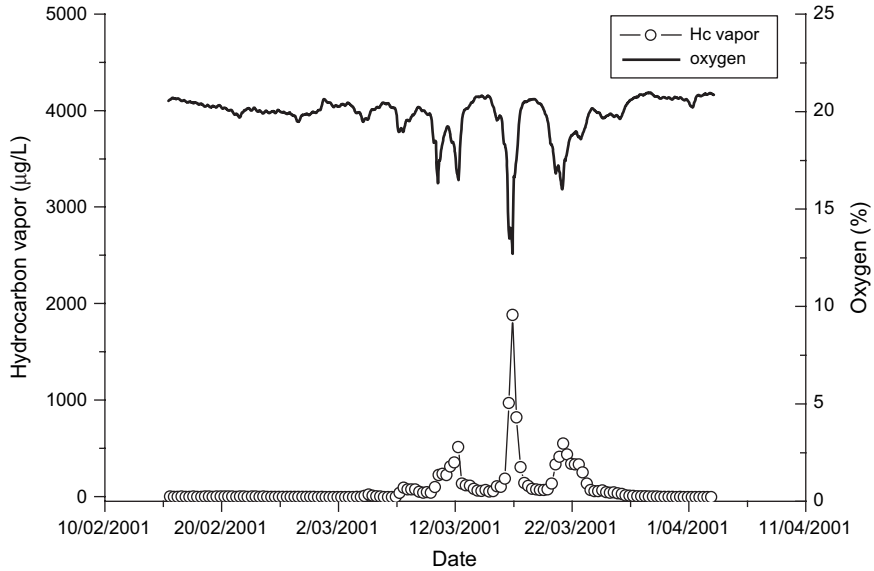


**Figure 6. Concurrent oxygen and hydrocarbon vapor concentration fluctuations from oxygen and VOC probes at a depth of 0.5 m at Site G.**

hydrocarbon vapor fluxes to the oxygen flux. If, however, we retain the fundamental aspects of this approach, which is that oxygen reacts instantaneously (or rapidly compared to transport times), then we can couple oxygen and hydrocarbon fluxes. Such an approach was first proposed in the American Petroleum Institute report by Roggemans et al. (2001) during their evaluation of soil-gas field data (for Behaviour A), and it was referenced in the three-dimensional modeling work of Abreu and Johnson (2006) in relation to the far field distribution of oxygen and vapors away from building foundations.

For this approach, consider steady-state hydrocarbon vapor diffusion from a constant concentration source $C_{H,max}$ at a depth $z = L_{max}$ at the base of the soil profile. Consider also oxygen diffusion from a constant maximum concentration $C_{Ox,max}$ at ground surface $z = 0$. Assume that the hydrocarbon vapors instantaneously react with oxygen at the depth $z = L$ and also decrease to zero at this location. Under these assumptions the simple equations for oxygen, $C_{Ox}(z)$, and hydrocarbon vapor, $C_H(z)$, concentrations become:

$$C_{Ox}(z) = C_{Ox,max}(1 - z/L) \quad (1)$$

$$C_H(z) = C_{H,max}\left[1 - (L_{max} - z)/(L_{max} - L)\right] \quad (2)$$

The balancing of fluxes at $z = L$ gives:

$$D_{Ox}C_{Ox,max}/L = \gamma D_H C_{H,max}/(L_{max} - L) \quad (3)$$

where $D_{Ox}$ is the oxygen diffusion coefficient, $D_H$ is the hydrocarbon vapor diffusion coefficient, and $\gamma$ is the stoichiometric mass of oxygen consumed per mass of hydrocarbon consumed in the biodegradation reaction. Rearranging, we can define the depth L as

$$L = L_{max}/(1 + 1/\eta) \quad (4)$$

where $\eta = D_{Ox}C_{Ox,max}/(\gamma D_H C_{H,max})$ measures the undersupply of oxygen flux ($\eta < 1$, $L/L_{max} \rightarrow 0$) or oversupply of oxygen flux ($\eta > 1$, $L/L_{max} \rightarrow 1$) with respect to the hydrocarbon flux. If all assumptions are valid, the model requires only a priori knowledge of the maximum oxygen and hydrocarbon concentrations, their diffusion coefficients, and the stoichiometry of the hydrocarbon biodegradation reaction. Note that for layered soils, $D_{Ox}$ and $D_H$ may be replaced with effective diffusion coefficients calculated according to the usual harmonic averaging method (e.g., Crank 1975, p. 267).

Example model profiles using Equations 1, 2, and 4 are shown in Figure 7. Note that the instantaneous model profiles are predicted fits using the model described previously rather than best fits to measured profiles. Table 3 gives measurements and model estimates of the depths L where oxygen and hydrocarbon concentrations decrease to zero. The model estimates of L are comparable to those measured, except in the fill at Site D and for the winter profile at Site B, both of which have nonuniform diffusion coefficients over the depth profiles. In particular, the fill area at Site D had a compacted clay layer at 0.5 to 1 m below ground, and Site B had a thin shallow soil layer with high soil moisture content in winter that was controlling the net fluxes of oxygen and hydrocarbon vapors (Davis et al. 2005). The accuracy of the measured estimate for L is strongly controlled by the spatial interval of measurements over the depth profile and, as pointed out earlier, possibly the sampling and measurement technique used (compare Figures 2 and 4). Estimates of L were also calculated using the free air diffusion coefficients ($D_{free}$) to compare to L values derived using the effective diffusion coefficients ($D_{eff}$) obtained from $\theta_T$ and $\theta_a$ (Table 3). Only minimal differences in the estimated $D_{eff}$ and $D_{free}$ values of L were

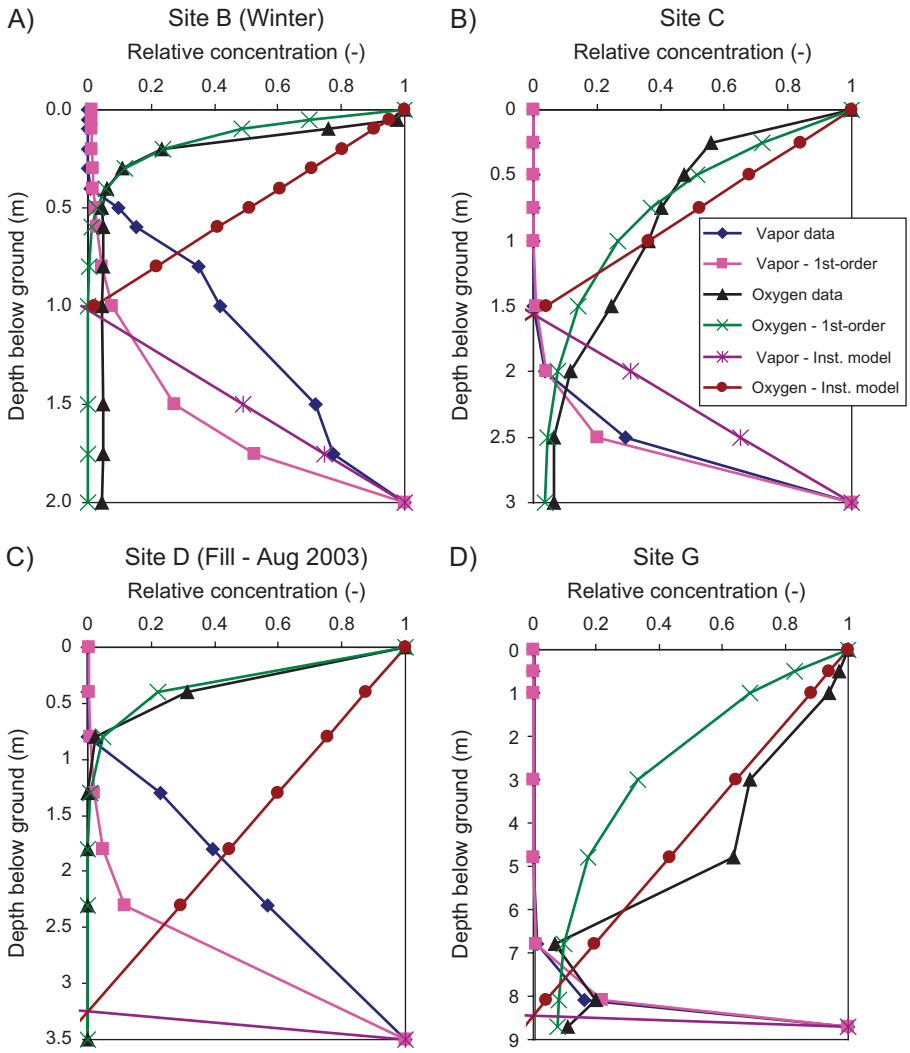


**Figure 7. Oxygen and hydrocarbon vapor depth profiles from manual sampling compared to the predictions from the instantaneous linear model and the best fits to the first-order model.**

observed with the exception of Sites B, E, and G. This indicates, because L is calculated from the ratio of the oxygen and hydrocarbon vapor diffusion coefficients, that knowledge of $\theta_T$ and $\theta_a$, and hence $D_{eff}$, for determining L using the instantaneous model approach may not be essential at the majority of the sites investigated in this study.

Adopting an alternate empirical estimate of the diffusion coefficient, other than that proposed by Millington and Quirk (1961), may alter the $D_{Ox,eff}$ to $D_{H,eff}$ ratio, especially where the air-filled or the total porosities change significantly from the shallow to deeper zones of the soil profile. Additionally, the stoichiometry coefficient (taken as 3.5 here) varies with the type of hydrocarbon compound, although the variation is not great; see Baker et al. (2000) or DeVaull (2007) for a generalized approach.

## First-Order Model and Rates

As indicated earlier, the oxygen and vapor concentration depth profiles observed at these field sites were most often linear or near linear with depth (see Table 2 and example depth profiles in Figures 1 and 7). Effectively, this can occur only when most of the degradation occurs at the depth of the near-minimum oxygen and hydrocarbon vapor concentrations and when degradation rates are low through the remainder of the soil profile. Assumptions of oxygen consumption at shallower depths of the soil profile, or hydrocarbon vapor degradation at greater depths of the profile, using either first- or zero-order biodegradation rates, would lead to nonlinear depth profiles and overlapping depth profiles if biodegradation rates are low.

To illustrate this further, steady-state first-order biodegradation models were fitted to each of the 13 depth profiles for both oxygen and hydrocarbon vapor. In this case the oxygen and hydrocarbon vapor concentrations were modeled independently. For oxygen, the concentration at ground surface was assumed to be a maximum (i.e., $C_{Ox} = C_{Ox,max}$ at $z = 0$) and the oxygen flux at some depth $L_{max}$ was assumed to be zero (i.e., $dC_{Ox}/dz = 0$ at $z = L_{max}$). $C_{Ox,max}$ can be set equal to the concentration in the atmosphere above ground ($2.79 \times 10^5$ μg/L) or a lower concentration observed beneath a building or covered area. The depth $L_{max}$ could be the top of the capillary fringe of the

**Table 3**
**Measured and Estimated Depths and Estimated Liquid Phase First-Order Hydrocarbon Vapor Degradation Rates**

| Site | Location or Date | Measured Depth L (m) | | Estimated L from Equation 4 (m) [1] | | Liquid-Phase Hydrocarbon Vapor Degradation Rates ($h^{-1}$) | |
|---|---|---|---|---|---|---|---|
| | | From oxygen data | From vapor data | Using $D_{eff}$ values[2] | Using $D_{free}$ values[3] | Aliphatic[4] | Aromatic[4] |
| **A** | Open ground | 2.50<L <2.75 | 2.25<L <2.50 | 2.5 | 2.5 | 61 | 0.24 |
| **A** | Under building | 0 | N/A | N/A | | 1.1 | 0.0046 |
| **B** | Summer | ~1.5 | 1.25<L<1.5 | 1.2 | 1.7 | 180 | 0.69 |
| **B** | Winter: wet layer | ~0.5 | 0.4 | 1.0 | 1.6 | 12 | 0.048 |
| **C** | Open ground | 2.5 | 1.5 | 1.6 | 1.5 | 8.9 | 0.035 |
| **D** | Fill: clay layer Aug 2003 | 0.8 | 0.8 | 3.3 | 3.2 | 3.0 | 0.012 |
| **D** | Fill: clay layer May 2004 | 0.8 | 0.8 | 2.2 | 2.2 | 6.1 | 0.024 |
| **D** | Verge Aug 2003 | 1.25<L <2.25 | 1.25<L <2.25 | 2.1 | 2.2 | 8.6 | 0.033 |
| **D** | Verge May 2004 | ~1.3 | <0.8 | 1.3 | 1.3 | 5.3 | 0.021 |
| **E** | Beside a building | 1.0<L<1.5 | 1.0<L<1.5 | 1.5 | 1.2 | 0.005 | 0.000020 |
| **F** | Apr 2002 | 5.0 | 3.0<L<5.0 | 4.6 | 4.8 | 0.30 | 0.0012 |
| **F** | Oct 2002 | 5.0 | 3.0<L<5.0 | ~5 | 5 | 0.22 | 0.00087 |
| **G** | Open ground | ~8.7 | 6.8<L<8.1 | 8.5 | 6.4 | 0.02 | 0.000078 |

[1]Assumes $\gamma = 3.5$ g oxygen per gram of hydrocarbon vapor.
[2]Using $D_{Ox,eff}$ and $D_{H,eff}$ as shown in Table 2.
[3]Calculated using $D_{Ox,free}=2.01 \times 10^{-5}$ $m^2/s$ (Gliński and Stępniewski 1985), $D_{H,free}=8 \times 10^{-6}$ $m^2/s$ (Grathwohl 1998).
[4]Aliphatic values are determined by assuming the Henry's Law coefficient is 59, being the maximum of the range in DeVaull (2007). Aromatic values are determined by assuming the benzene Henry's Law coefficient is 0.23 (DeVaull 2007).

water table or the top of the vapor source zone. We could have also assumed a zero oxygen concentration at depth $L_{max}$, but this would constrain the oxygen concentration to be zero at that depth even when, in the most general case, degradation (oxygen consumption) might be zero. The equation for the oxygen concentration depth profile becomes (see Appendix A):

$$C_{Ox}(z) = C_{Ox,max}\cosh\left[k_{Ox}(L_{max} - z)\right]/\cosh(k_{Ox}L_{max}) \quad (5)$$

where $\cosh(z) = (e^z + e^{-z})/2$, $k_{Ox} = (R_{Ox}/D_{Ox})^{1/2}$, and $R_{Ox}$ is the first-order oxygen consumption rate.

Likewise, for hydrocarbon vapors emanating from a constant source of concentration $C_{H,max}$ at depth $L_{max}$, having a zero flux at the ground surface and a first-order degradation rate $R_H$, we can write the equation for the hydrocarbon vapor concentration depth profile as:

$$C_H(z) = C_{H,max}\cosh(k_H z)/\cosh(k_H L_{max}) \quad (6)$$

where $k_H = (R_H/D_H)^{1/2}$. Here, we could have set the vapor concentration to zero at the ground surface if open ground conditions were prevalent. For the 13 profiles this is a common occurrence, but for open ground conditions the vapors rarely penetrate close to the ground surface, so a zero flux condition instead seems reasonable. Also, adopting a zero flux condition frees the concentration at ground surface to vary, which allows the potential for accumulation of vapors beneath a built structure, although theoretically no exchange with a built structure is allowed for in this analysis.

Equations 5 and 6 were fitted to the 13 hydrocarbon and oxygen depth profiles. The fitting was carried out manually to ensure that the fitted curve approximated the depth where the measured hydrocarbon concentration was at or below detection limits. This is a best fit to the profile data, in contrast to the instantaneous model, which is a predictive estimate based on maximum concentrations at surface and depth. Examples are given for Sites B (Winter), C, D (Fill Aug. 2003), and G in Figure 7. Similar fits were obtained for the other profiles. Of those shown in Figure 7, the first-order model fit is good for oxygen profiles at Sites B, C, and D, but poor at Site G. The fit to hydrocarbon vapor profiles is good at Sites G and C, but poor at B and D. Liquid-phase first-order hydrocarbon vapor degradation rates estimated from these fits are summarized in Table 3. These are obtained by multiplying the gas phase degradation rate $R_H$ by the ratio of the dimensionless Henry's law constant and the average water-filled porosity (determined from $\theta_T$ and $\theta_a$). Water–filled porosities were variable between sites but reasonably uniform with depth, especially in the sandy soils. The average water-filled porosities used were quite large, ranging from 0.11 to 37 $m^3/m^3$, except for the lowest average. The lowest average value was 0.06 $m^3/m^3$ for a sandy site that had this moisture content throughout the soil profile. The Henry's Law constants were taken to be typical of the maximum of the range for aromatic and aliphatic hydrocarbons (see DeVaull 2007).

Across all sites and locations, the aliphatic hydrocarbon first-order degradation rates range from $5.0 \times 10^{-3}$ to 180 $h^{-1}$ with a geometric mean of 2.0 $h^{-1}$. The aromatic hydrocarbon first-order degradation rates range from 2 ×

$10^{-5}$ to 0.69 $h^{-1}$ with a geometric mean of $7.8 \times 10^{-3}$ $h^{-1}$. From an extensive dataset, DeVaull (2007) quotes a geometric mean liquid-phase first-order reaction rate of 71 $h^{-1}$ for aliphatics with a standard deviation range of 8 to 380 $h^{-1}$, and for aromatics a geometric mean of 0.79 $h^{-1}$ with a standard deviation range of 0.06 to 10 $h^{-1}$. Apart from Site B (Summer), all values determined in this study are below the geometric mean for aliphatics quoted by DeVaull (2007) and all are below the geometric mean for aromatics (standardized to benzene). Only Site A (open ground) and Site B (Summer) had aromatic degradation rates that were above the minimum range of the standard deviation, whereas additionally Sites C and Site D (Verge, August 2003) had aliphatic degradation rates that were above the minimum range of the standard deviation quoted by DeVaull (2007).

## Integration of Results and Conclusions

Overall, in comparison to the pseudo first-order rates reported by DeVaull (2007), the hydrocarbon vapor degradation rates determined across the 13 profiles in this study appear to be low. It might be expected for such low degradation rates that oxygen and vapor concentration profiles would overlap and that vapors might persist to shallower depths. This is not the case across all 13 profiles, except at Site A under the building, and indeed the rates of degradation in these profiles are high relative to the potential for hydrocarbon vapors to diffuse through the soil to the ground surface. As discussed earlier, for all but a very few data points, there was rarely oxygen detected in the zone where hydrocarbon vapors were detected and little or no overlap was observed.

The instantaneous model structure avoids the need for rate estimates. It offers a simple and perhaps conservative way to incorporate biodegradation into vapor intrusion assessment. For example, Johnson and Ettinger (1991) embody $Q_{soil}$, the advective building foundation air exchange rate into their model solution. This delivers vapors into the building via advective pressure driven air flow. DeVaull (2007) expands its application to also include oxygen flux into the subsurface in his oxygen-limited approach. Using this approach and taking the typical range quoted for $Q_{soil}$ as 1 to 10 L/min, assuming $C_{Ox,max}=2.79 \times 10^5$ μg/L, and the typical surface area of a building foundation as $A_b =$ 100 $m^2$ (DeVaull 2007), gives an advective flux of oxygen into the soil of $J_{Ox,Qsoil} = Q_{soil}C_{Ox,max}/A_b = 2800$ to 28,000 μg/$m^2$/min. The diffusive flux of oxygen $J_{Ox,D}$ into the soil profile is given by $J_{Ox,D} = D_{Ox}C_{Ox,max}/L = 110$ to 44,000 μg/$m^2$/min, assuming $D_{Ox}$ spans the range in Table 2 and $L = L_{max} = 1$ to 10 m. For small $Q_{soil}$, high $\theta_a$, or small L values, the diffusive flux of oxygen is up to an order of magnitude greater than the advective flux of oxygen, but for large $Q_{soil}$, low $\theta_a$, or large L values, the diffusive flux of oxygen may be orders of magnitude less than the advective flux.

Even when $Q_{soil}$ is large, diffusion operates and, as seen in Figure 6, assuming a constant or average $Q_{soil}$ may not be appropriate given the responses of oxygen and vapor pressures to transient effects in this shallow zone of the soil profile. Setting the advective flux of oxygen to zero by setting $Q_{soil}$ to zero (only for oxygen) and estimating the oxygen flux solely from the diffusive flux offers a possible conservative way of estimating the potential for aerobic biodegradation of the petroleum hydrocarbon vapors. For all the profiles investigated in this study (except Site A under the building where $C_{Ox,max} = 0$) the diffusive oxygen flux ranges from 220 to 13,000 μg/$m^2$/min, assuming $L_{max} =$ L. Note that L is usually much less than $L_{max}$, but using $L_{max}$ provides a lower and conservative diffusive flux estimate. Also, $L_{max}$ is already known if a standard Johnson and Ettinger (1991) vapor intrusion assessment is to be carried out at a site. Stoichiometrically, this diffusive oxygen flux can be used to estimate the flux reduction factor (FRF) (DeVaull et al. 2002) or the reduced net flux of hydrocarbon vapors moving toward a building. At these seven sites this reduction amounts to between 60 and 3700 μg/$m^2$/min. To apply this approach with confidence, the instantaneous model would need to be combined with field data to inform the model as to the presence and concentration of oxygen in the soil profile, as recommended by others such as Johnson et al. (1999). Otherwise, apart from perhaps $D_{Ox}$, all other parameters used by the model ($L_{max}$, $D_H$, $C_{H,max}$) are already required to carry out a standard vapor intrusion assessment using the Johnson and Ettinger (1991) approach, and the additional rate constants (e.g., $R_H$ or $R_{Ox}$) are not required; again, to be conservative, only diffusive oxygen flux from the surface would be assumed, with $Q_{soil}$ only applied to the movement of hydrocarbon vapors into a building.

Built structures will alter oxygen concentrations that may be observed under a building compared to that observed beside a building, as shown in Figures 1A and 1B, and see Abreu and Johnson (2006) or Patterson and Davis (2009). In this case, lateral migration of oxygen beneath a building foundation can be approximated in a similar way to that proposed in Equations 1, 2, and 3. An additional parameter value required is the slab or foundation dimension, but again this is a required parameter for a vapor intrusion assessment in any case.

There are a number of shortcomings in the simple assessment reported here. It assumes uniform nontransient conditions, constant and uniform diffusion coefficients, no advective flux of oxygen or hydrocarbon vapors, and instantaneous reaction of oxygen and hydrocarbon vapors. In addition, this approach assumes that oxygen and vapors migrate in one dimension, which is not the case when the ground is covered by a building (Abreu and Johnson 2005, 2006; Patterson and Davis 2009). Together with nonuniform diffusion coefficients, oxygen consumption by natural organic matter or other reduced species (Johnston and Desvignes 2003; DeVaull 2007) will also create nonlinear distributions of oxygen through the soil profile. This would serve to reduce the oxygen concentration in the soil profile both in reality and in a model informed by oxygen concentration data from the field. Inhibitive effects may also slow aerobic microbial biodegradation, which can create overlapping profiles, although high concentrations at the seven sites investigated in this study did not seem to create such inhibitions. In addition, the built environment changes the flux of oxygen and vapors, so that vapors may accumulate as in Figure 1A.

Some of these shortcomings are common to all currently available vapor intrusion assessment models. Despite this, the data presented here indicate that the kinetics or rates of the biodegradation reactions between oxygen and hydrocarbon vapors are not critical to the assessment of steady petroleum vapor transport, and that oxygen-limited instantaneous consumption of petroleum hydrocarbon vapors allows a simplified approach to vapor intrusion assessment. Combined with field measurement of the presence of oxygen in the subsurface, which will alleviate some uncertainty related to the shortcomings indicated above, the oxygen-limited instantaneous model offers the potential to reduce the complexity of initial petroleum hydrocarbon vapor intrusion assessments whilst taking some account of aerobic biodegradation processes.

## Acknowledgments

Many colleagues at the Commonwealth Scientific and Industrial Research Organisation (CSIRO) (John Rayner, David Briegel, Blair Robertson, Andrew Furness, Steve Fisher, Trevor Bastow, Robert Woodbury) assisted with the field studies reported here. The work was partially supported by BP, the Western Australian Department of Environment and Conservation, and the Cooperative Research Centre for Contamination Assessment and Remediation of the Environment and delivered through the CSIRO Water for Healthy Country National Flagship. Thanks too to George DeVaull and Ian Hers for discussions regarding vapor behaviors. Anonymous reviewers are also thanked for their comments on the paper.

## Appendix A: Derivation of Equation 5

We consider steady diffusion in a finite domain $z \in [0,L]$. Let the vapor concentration at location $z$ be denoted by $C(z)$. The (uniform) diffusion coefficient is $D$ and the irreversible rate of reaction (biodegradation) of the vapor is $R$ such that

$$D\frac{d^2C}{dz^2} - RC = 0 \tag{A.1}$$

i.e., $R$ represents first-order reaction kinetics. Defining $k = (R/D)^{1/2}$, the general solution to Equation A.1 can be expressed simply as

$$c(x) = Ae^{kx} + Be^{-kx} \tag{A.2}$$

where $A$ and $B$ are integration constants to be fixed by the application of boundary conditions. For the problem of interest here, we apply the conditions $C(0) = C_0$, i.e., concentration is constant at the ground surface, and $C'(L) = 0$, i.e., concentration flux is zero at $z = L$. Requiring Equation A.2 to satisfy these conditions yields the pair of simultaneous equations

$$\begin{aligned} A + B &= C_0 \\ kAe^{kL} - kBe^{-kL} &= 0 \end{aligned} \tag{A.3}$$

Solving Equation A.3 yields $A = C_0/(1 + e^{2kL})$ and $B = A\,e^{2kL}$. Substituting these expressions in Equation A.2, identifying $(e^z + e^{-z})/2$ with $\cosh(z)$, and rearranging yields the form of Equation 5.

## References

Abreu, L.D.V., and P.C. Johnson. 2006. Simulating the effect of aerobic biodegradation on soil vapor intrusion into buildings: Influence of degradation rate, source concentration and depth. *Environmental Science and Technology* 40, no. 7: 2304–2315.

Abreu, L.D.V., and P.C. Johnson. 2005. Effect of vapor source-building separation and building construction on soil vapor intrusion as studied with a three-dimensional numerical model. *Environmental Science and Technology* 39, no. 12: 4550–4561.

Baehr, A.L., and R.J. Baker. 1995. Use of a reactive gas transport model to determine rates of hydrocarbon biodegradation in unsaturated porous media. *Water Resources Research* 31, no. 11: 2877–2882.

Baker R.J., A.L. Baehr, and M.A. Lahvis. 2000. Estimation of hydrocarbon biodegradation rates in gasoline-contaminated sediment from measured respiration rates. *Journal of Contaminant Hydrology* 41: 175–192.

Crank, J.H. 1975. *The Mathematics of Diffusion*, 2nd ed. Oxford, UK: Clarendon Press.

Davis, G.B., M.G. Trefry, and B.M. Patterson. 2008. Petroleum vapour model comparison: Interim report for CRC CARE. Technical Report no. 1. Adelaide, Australia: CRC for Contamination Assessment and Remediation of the Environment.

Davis, G.B., J.L. Rayner, M.G. Trefry, S.J. Fisher, and B.M. Patterson. 2005. Measurement and modelling of temporal variations in hydrocarbon vapor behavior in a layered soil profile. *Vadose Zone Journal* 4, no. 2: 225–239.

Davis, G.B., M.G. Trefry, J. Öhman, and J.L. Rayner. 2001. Nitrogen flushing field experiments to determine the natural biodegradation of gasoline vapours in a sandy vadose zone. In *Proceedings of the First European Bioremediation Conference*, Chania-Crete, Greece, July 2–5: 9–12. Technical University of Crete, Greece.

Davis, G.B., T.R. Power, D. Briegel, and B.M. Patterson. 1998. BTEX vapour biodegradation rates in the vadose zone—Initial estimates. In *Groundwater Quality: Remediation and Protection*, Proceedings GQ'98 Conference, Tübingen, Germany, September 1998, ed. M. Herbert and K. Kovar, 300–303. IAHS Publ. 250. Wallingford, UK: International Association of Hydrological Sciences.

Davis, G.B., and A.I.M. Ritchie. 1986. A model of oxidation in pyritic mine wastes. Part 1: equations and approximate solution. *Applied Mathematical Modelling* 10, no. 5: 314–322.

DeVaull, G.E. 2007. Indoor vapor intrusion with oxygen-limited biodegradation for a subsurface gasoline source. *Environmental Science and Technology* 41, no. 9: 3241–3248.

DeVaull, G.E., R. Ettinger, and J. Gustafson. 2002. Chemical vapor intrusion from soil or groundwater to indoor air: Significance of unsaturated zone biodegradation of aromatic hydrocarbons. *Soil and Sediment Contamination* 11, no. 4: 625–641.

Franzmann, P.D., L.R. Zappia, T.R. Power, G.B. Davis, and B.M. Patterson. 1999. Microbial mineralisation of benzene and characterisation of microbial biomass in soil above hydrocarbon-contaminated groundwater. *FEMS Microbial Ecology* 30: 67–76.

Gliński J., and W. Stępniewski. 1985. *Soil Aeration and Its Role for Plants*. Boca Raton, Florida: CRC Press Inc.

Golder Associates. 2008. Evaluation of vadose zone biodegradation of petroleum hydrocarbons: Implications for vapour intrusion guidance. Final draft report. Research study for Health Canada and Canadian Petroleum Products Institute. British Columbia: Burnaby.

Grathwohl, P. 1998. *Diffusion in Natural Porous Media: Contaminant Transport, Sorption/Desorption and Dissolution Kinetics*. Boston: Kluwer Academic Publishers.

Hers, I., R. Zapf-Gilje, P.C. Johnson, and L. Li. 2003. Evaluation of the Johnson and Ettinger model for prediction of indoor air quality. *Ground Water Monitoring and Remediation* 23, no. 1: 62–76.

Hers, I., J. Atwater, L. Li, and R. Zapf-Gilje. 2000. Evaluation of vadose zone biodegradation of BTX vapours. *Journal of Contaminant Hydrology* 46: 233–264.

Höhener, P., C. Duwig, G. Pasteris, K. Kaufmann, N. Dakhel, and H. Harms. 2003. Biodegradation of petroleum vapors: Laboratory studies on rates and kinetics in unsaturated alluvial sand. *Journal of Contaminant Hydrology* 66: 93–115.

Johnson, P.C., M.W. Kemblowski, and R.L. Johnson. 1999. Assessing the significance of subsurface contaminant vapor migration to enclosed-spaces: Site-specific alternatives to generic estimates. *Journal of Soil Contamination* 8, no. 3: 389–421.

Johnson, P.C., and R.A. Ettinger. 1991. Heuristic model for predicting the intrusion rate of contaminant vapors into buildings. *Environmental Science and Technology* 25, no. 8: 1445–1452.

Johnston, C.D., and A. Desvignes. 2003. Evidence for biodegradation of dissolved petroleum hydrocarbons during in situ air sparging in large laboratory columns. *Water, Air and Soil Pollution: Focus* 3: 25–33.

Lahvis, M.A., and A.L. Baehr. 1996. Estimation of rates of aerobic hydrocarbon biodegradation by simulation of gas transport in the unsaturated zone. *Water Resources Research* 32, no. 7: 2231–2249.

Lundegard, P.D., P.C. Johnson, and P. Dahlen. 2008. Oxygen transport from the atmosphere to soil gas beneath a slab-on-grade foundation overlying petroleum-impacted soil. *Environmental Science and Technology* 42, no. 15: 5534–5540.

Miller, R.N., C.C. Vogel, and R.E. Hinchee. 1991. A field-scale investigation of petroleum hydrocarbon biodegradation in the vadose zone enhanced by soil venting at Tyndall Air Force Base, Florida. In *In Situ Bioreclamation: Applications and Investigations for Hydrocarbon and Contaminated Site Remediation*, ed. R.E. Hinchee and R.F. Olfenbuttel, 283–302. Newton, Massachusetts: Butterworth-Heinemann.

Millington, R.J., and J.P. Quirk. 1961. Permeability of porous solids. *Transactions of the Faraday Society* 57: 1200–1207.

Öhman, J. 1999. Modelling transport and degradation dynamics of BTEX vapours in a contaminated vadose zone. Master's thesis, School of Engineering, Uppsala University, Sweden.

Ostendorf, D.W., T.H. Schoenberg, E.S. Hinlein, and S.C. Long. 2007. Monod kinetics for aerobic biodegradation of petroleum hydrocarbons in unsaturated soil microcosms. *Environmental Science and Technology* 41, no. 7: 2343–2349.

Ostendorf, D.W., and D.H. Kampbell. 1991. Biodegradation of hydrocarbon vapors in the unsaturated zone. *Water Resources Research* 27, no. 4: 453–462.

Patterson, B.M., and G.B. Davis. 2008. An in situ device to measure oxygen in the vadose zone and in groundwater: Laboratory testing and field evaluation. *Ground Water Monitoring and Remediation* 28, no. 2: 68–74.

Patterson, B.M., and G.B. Davis. 2009. Quantification of vapour intrusion pathways into a slab-on-ground building under varying environmental conditions. *Environmental Science and Technology* 43, no. 3: 650–656.

Patterson, B.M., G.B. Davis, and A.J. McKinley. 2000. Volatile organic compounds in groundwater, probes for the analysis of. In: *Encyclopedia of Analytical Chemistry: Instrumentation and Application*, ed. R.A. Meyers, 3515–3526. New York: John Wiley and Sons Ltd.

Ririe, G.T., R.E. Sweeney, and S.J. Daugherty. 2002. A comparison of hydrocarbon vapour attenuation in the field with predictions from vapour diffusion models. *Soil and Sediment Contamination* 11, no. 4: 529–554.

RISC. 2006. Risk-integrated software for clean-ups. Version 4.05 – July 2006. http://www.groundwatersoftware.com/risc.htm (accessed July 1, 2008).

Ritchie, A.I.M. 1977. Heap leaching: A gas diffusion rate-limited model. AAEC/E429. Sydney, Australia: Australian Atomic Energy Commission.

Roggemans, S., C.L. Bruce, P.C. Johnson, and R.L. Johnson. 2001. Vadose zone natural attenuation of hydrocarbon vapors: An empirical assessment of soil gas vertical profile data. Bulletin No. 15. Washington, D.C.: American Petroleum Institute.

Trefry, M.G., J. Öhman, and G.B. Davis. 2001. A simple numerical approach for assessing coupled transport processes in partitioning systems. *Applied Mathematical Modelling* 25, no. 6: 479–498.

Trefry, M.G., J. Öhman, D.S. Whyte, and G.B. Davis. 2000. A time-synchronous domain decomposition code for multiphysics systems. CTAC99, The 9th Biennial Computational Techniques and Applications Conference and Workshops, ANU, Canberra. *Australian & New Zealand Institute of Applied Mathematics (ANZIAM) Journal* 42(E), C1443–C1464.

Turczynowicz, L., and N.I. Robinson. 2001. A model to derive soil criteria for benzene migrating from soil to dwelling interior in homes with crawl spaces. *Human and Ecological Risk Assessment* 7, no. 2: 387–415.

USEPA. 2002. Draft guidance for evaluating the vapor intrusion to indoor air pathway from groundwater and soils (Subsurface vapor intrusion guidance). EPA 530-D-02-004. Washington, D.C.: U.S. Environmental Protection Agency, Office of Solid Waste and Emergency Response.

## Biographical Sketches

***Gregory B Davis**, Ph.D., corresponding author, is a chief research scientist with CSIRO Land and Water and adjunct professor in the School of Earth and Environment, University of Western Australia. He can be reached at Private Bag No. 5, Wembley WA 6913, Australia; (61) 8-93336386; fax (61) 8-93336211; Greg.Davis@csiro.au.*

***Bradley M Patterson**, Ph.D., is a principal research scientist with CSIRO Land and Water, Private Bag No. 5, Wembley WA 6913, Australia; (61) 8-93336276; fax (61) 8-93336211; Bradley.Patterson@csiro.au.*

***Michael G Trefry**, Ph.D., is a principal research Scientist with CSIRO Land and Water and adjunct research fellow in the School of Earth and Environment, University of Western Australia. He can be reached at Private Bag No. 5, Wembley WA 6913, Australia; (61) 8-93336286; fax (61) 8-93336211; Mike.Trefry@csiro.au.*